



## Estimation of travel time of P- and S-waves in and around Sylhet and Mat faults in Surma Basin, northeast India

Saitluanga<sup>1\*</sup>, R. P. Tiwari<sup>2</sup> and Saurabh Baruah<sup>3</sup>

<sup>1</sup> Department of Geology, Pachhunga University College, Aizawl 796001, India

<sup>2</sup> Department of Geology, Mizoram University, Aizawl 796004, India

<sup>3</sup> Geoscience Divisions, CSIR North East Institute of Science and Technology, Jorhat 785006, Assam, India

Received 29 April 2014 | Revised 23 May 2014 | Accepted 30 May 2014

### ABSTRACT

A regional seismicity map for Surma valley and the adjoining region, covering the area bounded by longitudes 90-95°E and latitude 22-26°N was prepared covering the period between 1969-2009 over the generalized tectonic map of the region. The best estimation of hypocentral parameters form the prime input for the estimation of travel time of P- and S- waves of any region. The Riznichenko diagrams clearly show the change in shape of the travel time versus distance with increasing focal depth, indicative of both a geometrical effect and an increasing P-wave velocity. The Wadati diagrams show systematic decrease in  $t_s/t_p$ , suggesting that the velocity for shear waves increases faster than that for the compressional waves in the upper levels of the crust.

**Key words:** Epicenter; HYPOCENTER; Riznichenko method; travel time; Wadati plot.

### INTRODUCTION

The fundamental data for seismological studies of the earth's interior are the travel times of seismic waves. The measurements available are the arrival times of seismic waves at receivers. To convert these to travel times, the origin time and location of the source must be known.<sup>1</sup> These parameters, which are known for artificial sources, must be estimated from the observations of earthquake sources. Hence travel time

data include information about both the source and the properties of the medium, and separating the two is a challenge in many seismological studies. The travel times are used to learn about the velocity structure within the source and the receiver. In general waves follow paths that depend on the velocity structure.<sup>1</sup> Hence the structure through which waves travelled must be known. To illustrate these the travel time between two points are considered and the velocity could be found by dividing the distance by the travel time.

Travel times of P- and S-waves has significant role in earthquake seismology. The precise estimates of P- and S-waves travel time of local

Corresponding author: Saitluanga

Phone: +91-9436155837

E-mail: [stasailo@yahoo.com](mailto:stasailo@yahoo.com); [stasailo@gmail.com](mailto:stasailo@gmail.com)

earthquakes throws light on the regional crustal structure.<sup>2,5</sup> The travel time (T) versus epicentral distance ( $\Delta$ ) curve for P- and S-waves for different depth ranges always remain significant towards the estimation of velocity structure.

In 1930, Jeffreys, starting from the Zoppritz-Turner tables, inaugurated a series of successive approximations towards improved travel time table. In 1935 the first Jeffreys-Bullen tables were produced.<sup>6</sup> Substantial refinements were incorporated in a new set of 'JB' tables first published in 1940.<sup>7</sup> Compatible tables for near earthquake phases are also included. The tables are in a form which enables focal depth to be readily taken into account. The aim of the tables is to serve as a standard for the 'average' global earthquake.

Developments of modern seismology since the late 1980's have resulted in a large increase in seismological data and their accuracy. Recording of broadband seismic signals has allowed several reassessments of the long-used classic travel time tables of Jeffreys and Bullen (1940).<sup>7</sup> Discrepancies for these tables, although minor, were already pointed out by the authors. Moreover, the accuracy of source location today is incomparably greater than those that had been basis for the Jeffreys-Bullen tables.

Tandon (1954)<sup>2</sup> was the first to develop a crustal model from travel times for northeastern India regions. Subsequently, Saha *et al.* (1981)<sup>3</sup> and Gupta *et al.* (1982)<sup>4</sup> also proposed models. But it is a common experience that travels time for near earthquake phases vary from region to region because of regional variation in velocities. Moreover, crustal structure varies from region to region. Furthermore, the observed data will enable better and more accurate location of epicenters. The study region is seismically active because of complex geotectonic settings.<sup>8,9</sup> The occurrence of earthquakes in the basin extend an insight to the estimation of travels times of P- and S- waves and allows subsequent understanding of the in situ dynamics. This study attempts to estimate the travel time pattern of body waves in the eastern part and northern part of Surma valley and its vicinity. A comparison

of travel times with the findings of other studies are also made to revalidate the estimation. Details are highlighted here.

### *Tectonic Settings*

The basin is bounded on the north by the Shillong Plateau, east and southeast by the Chittagong-Tripura folded belt of the Indo-Burman ranges and the west by the Indian Shield platform (Figure 1). To the south and southwest it is open to the main part of the Bengal Basin. The topography is predominantly flat with some north-south trending ridges of twenty to several hundred meters elevation present in the northeastern border. The Bouguer anomaly map show gradual higher values (negative) towards the center of the basin. Mizoram lies in the Neogene Surma basin which is bounded by the post-Barail unconformity, subsequently faulted to the east; the E-W Dauki fault and NE-SW Disang thrust to the north and northeast; the NE-SW Sylhet fault and Barisal-Chandrapur high concealed below the alluvium of Bangladesh to the west and north-west.<sup>10</sup> To the south, the basin is extended up to the Arakan coastal area of Myanmar. Within this vast terrain of Surma valley lies Mizoram along with the states of Tripura, Cachar and Karimganj districts of Assam and western part of Manipur, Sylhet and Chittagong districts of Bangladesh and Arakan coastal zone of Myanmar. There are many NE lineaments/faults in Surma basin which show strike-slip displacement of the fold axes along them.. The two most striking and important faults are Mat fault, which runs across the state of Mizoram in NW-SE direction and Sylhet fault, which runs in NE-SW direction concealed beneath the alluvium of Bangladesh.

### *Data*

Seismicity map for the study area and adjoining regions was prepared by plotting the earthquake epicenters during the period 1969 to 2009 over the generalized tectonic map of the region forms the database for this study (Figure 1).The

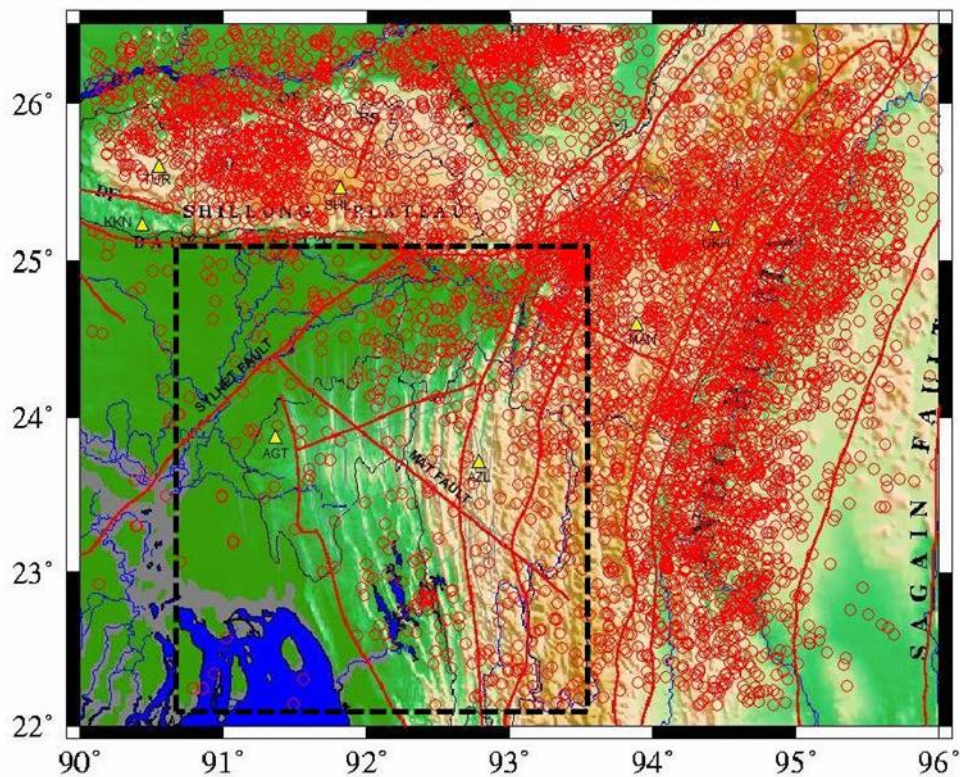


Figure 1. Relocated earthquakes in and around Surma valley. The rectangular box indicates the events within Surma valley.

area between 90°E and 95°E longitudes and 22° N and 26°N latitudes covering the region of this study experienced more than 2700 earthquake events over a span of 40 years. Re-computation of hypocenters of all the earthquakes occurring in the eastern part and northern part of Surma valley is done using HYPOCENTER program of Lienert *et al.*<sup>11</sup>

Using the arrival times of P- and S-waves of earthquakes and following the location algorithm package of Lienert *et al.*<sup>11</sup> hypocentral parameters are computed based on the crustal velocity model of Bhattacharyya *et al.*<sup>12</sup> for determining P-wave to S-wave velocity ratios. The study also utilizes the hypocenter data file compiled jointly by RRL/NEIST-Jorhat and NGRI-Hyderabad complemented by phase data from IMD-Shillong, IIG-Shillong, Manipur University, Gauhati University and Mizoram Univer-

sity. The accurate location stations and epicenters are the most important parameters towards this estimation of P- and S-wave travel times. The accrued and relocated database contains all these information.

## METHOD

A combination of the methods of Wadati,<sup>13</sup> Ryznichenko,<sup>14</sup> and Bune *et al.*<sup>15</sup> was used for estimation of upper crustal velocity structure. Data required for velocity analysis using these methods are P- and S-wave travel times to various recording stations for a number of earthquakes its epicentral locations and distances.

In the first step of the analysis, epicentral locations of more than 2700 earthquakes were estimated using the HYPOCENTER<sup>11</sup> hypocentral location program and an assumed velocity

model<sup>16</sup> (Fig. 2). This is because epicentral distances to recording stations are required for subsequent calculations. Also, estimates of epicentral coordinates are relatively insensitive to velocity models if an earthquake occurs within a recording array. This has been remarked by Nicholson and Simpson<sup>17</sup> likewise.

In the second step, Wadati method (Wadati)<sup>13</sup> has been used for getting model-independent estimates of travel times of P- and S-waves to various stations. From this estimates of the origin times of earthquakes as well as P- and S-wave travel time ratios were made. For this purpose, differences in arrival times of P- and S-phases were plotted against the P arrival time for each of the earthquakes. Figure 2 to 8 gives examples of Wadati and Riznichenko diagrams obtained during the analyses. Such diagrams are classified depending upon whether the outliers among the plotted points were within 0.5 standard deviation (SD), between 0.5 and 1.0 SD, or more than 1.0 SD, respectively.

In the next step of the analysis, the Riznichenko method<sup>14</sup> was used to estimate the focal depths of earthquakes and the vertical travel times of P and S phases between the respective hypocenters and epicenters. Squares of the travel times ( $t^2$ ) of either all the P or all the S phases from an earthquake are plotted against the squares of epicentral distances ( $x^2$ ) of respective stations. Such graphs are called Riznichenko diagrams. The square root of intercept ( $t_{pz}$  or  $t_{sz}$ ) on the  $t^2$  axis of such a plot is the required time of vertical travel of the P- or S-waves between the hypocenter and the epicenter. The square root of inverse of the slope of a least squares line fitted through the data points of a Riznichenko diagram when multiplied by a travel time, gives a focal depth estimate for that earthquake. Such focal depth estimates are denoted here as  $h_{riz}$ . Those point or points on such plots which were two standard deviation away from a least squares line, were excluded and then fitted in a line in a least squares sense through the remaining data points. The slope of this line was used to calculate  $h_{riz}$  in such cases.

A detailed description of the methodology is

given below:

#### *The Wadati's method*

The Method assumes that:

1. The Poisson's ratio along the ray paths for hypocenters to the recording station is constant, and
2. The P- and S-waves start at the same time from the source.

The two assumptions are reasonably appropriate. The method computes origin time of the earthquake and the ratio of the travel time of P- and S-wave independent of the physical model for the earth. The arrival time difference between S- and P-waves ( $T_s - T_p$ ) is plotted against the P arrival times. The plot contains data from all the network stations. For direct rays, a straight line fit occurs for the data. Due to reading inaccuracies and timing errors these are generally scattered and a least square fit is applied. The  $x$ -axis intercept is the origin time and is determined independent of the assumed velocity model. Slope of the line estimates the  $t_s/t_p$  (Figure 2a). The method is well suited for shallow focus local earthquakes.

#### *Riznichenko's Method*

To draw the Riznichenko's diagram, the travel time of waves to stations and the corresponding epicentral distances are required. With an initial location of earthquake and origin time computed from Wadati's method, travel time P- and S-waves are computed (Fig.2b)

Variation of  $t^2$  with  $x^2$  is plotted for a number of stations. A least square fit gives

$$t^2 = (x^2 + h^2)/v_e^2$$

Where  $v_e$  is the effective velocity  $h$  is the depth of focus, and  $x$  is the epicentral distance

The  $v_e^2$  so computed is neither the interval velocity nor simple average velocity.

In the final step of the analysis, the method of Bune *et al.*<sup>15</sup> a cumulative plot of the vertical travel times of P- and S-waves with respect to estimated focal depths for all the earthquakes

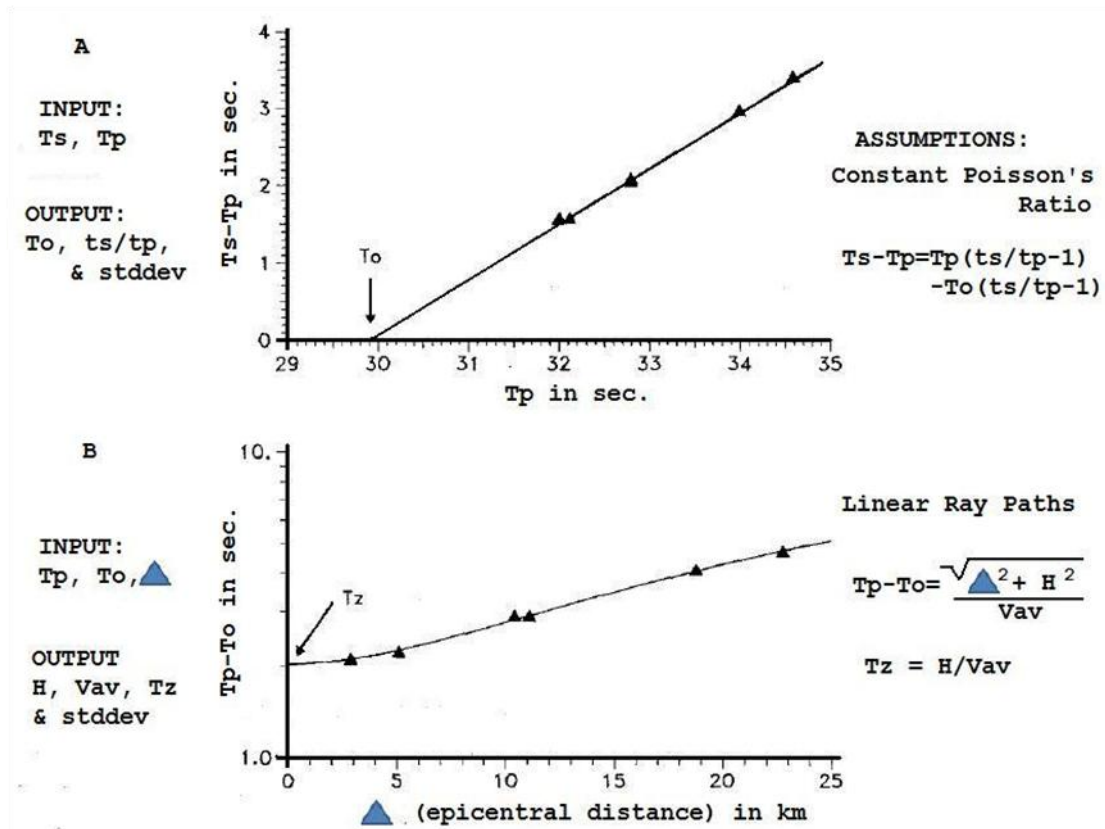


Figure 2. Equations and figures for (A) Wadati diagrams and (B) Riznichenko diagrams. To the left are input and output parameters, in the middle are the graphical forms, and to the right are the equations.

were obtained.

## RESULT AND DISCUSSION

The Wadati and Riznichenko diagrams plots are made for the events around Sylhet fault region in the northern part and Mat fault region in the eastern part of Surma valley. Figures (3 to 9) represent such relations for the P-travel times at each of the depths under consideration. The Riznichenko diagrams clearly show the change in shape of the travel time versus distance curve with increase in focal depth, indicative of both a geometrical effect and an increasing P-wave velocity. The Wadati diagrams show systematic decreases in  $t_s/t_p$ , suggesting that the velocity for shear waves increases faster than that for the compressional waves in the upper levels of the

crust. An interesting feature however, is the linearity of the Wadati diagrams. If  $t_s/t_p$  (and therefore  $V_p/V_s$ ) indeed changes with depth, the linear relation assumed in the Wadati diagram is no longer valid.<sup>18</sup> Yet it is apparent that, at close distances and shallow focal depths, the expected curvature of the Wadati diagram is not sufficiently resolvable with the available data. Summary of average half-space velocities for P- and S-waves calculated using the Riznichenko technique and values for  $t_s/t_p$  from the Wadati diagram are shown. Values shown are those data that are plotted as a function of focal depth for each individual earthquake.

Figure 3 shows that Wadati diagrams for eastern part of Surma valley and its vicinity are well constrained so far as the values of  $T_s - T_p$  vs.  $T_p$  and  $T_s - T_p$  vs.  $T_s$  are concerned. The  $T_s - T_p$

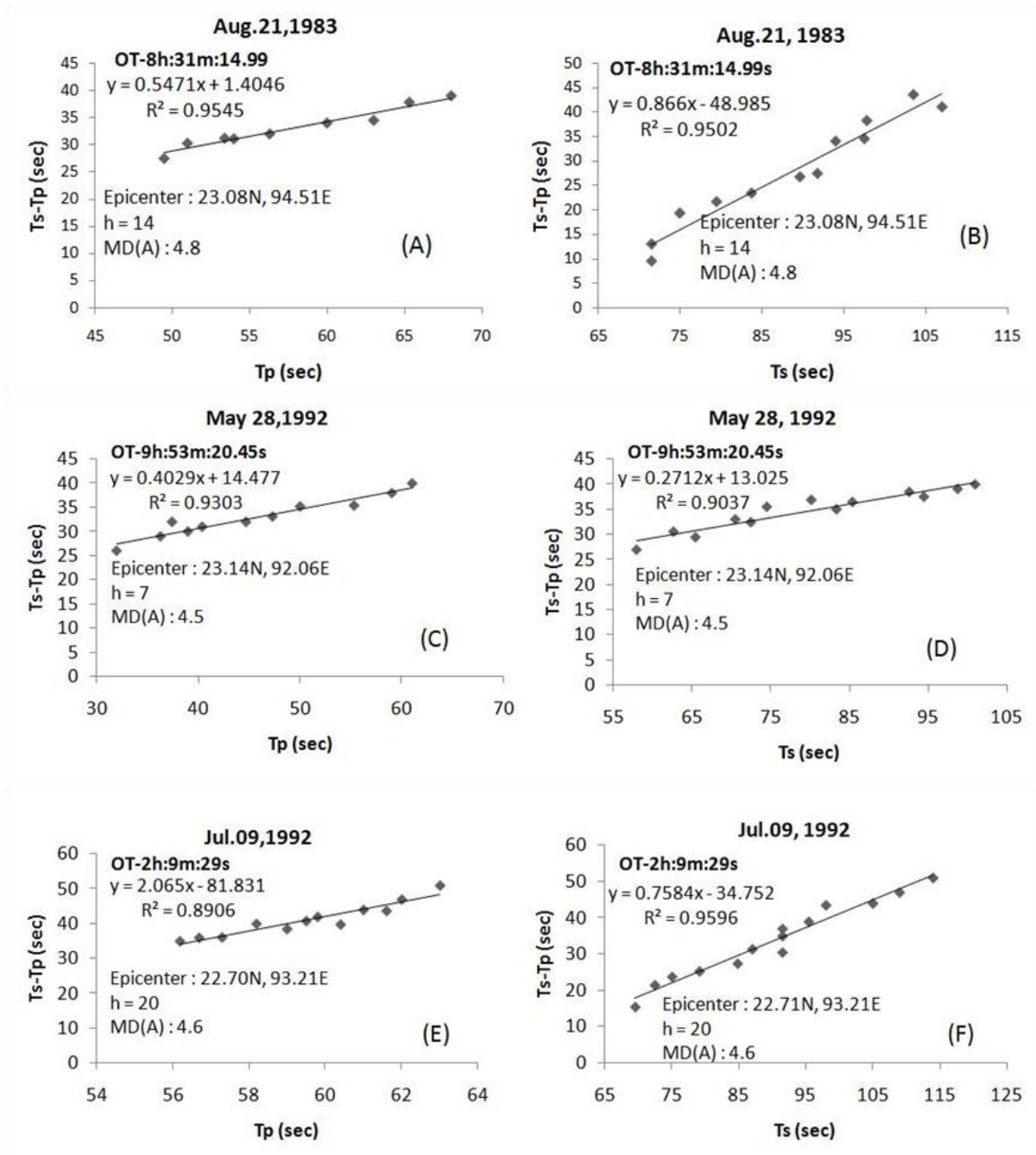


Figure 3. Wadati diagrams (A, B, C, D, E and F) for the earthquakes associated with events in the eastern part of Surma valley at depths (h) ranging between 0-20 km. Ts-Tp versus Tp and Ts-Tp versus Ts denote interval between the arrival time of P- and S-waves and arrival time of P- and S-waves at a seismic station respectively. Linear relations for the determination of P- and S-wave at a specific depth, involving Ts-Tp/Tp, Ts-Tp/Ts and origin time (O.T) are also shown.

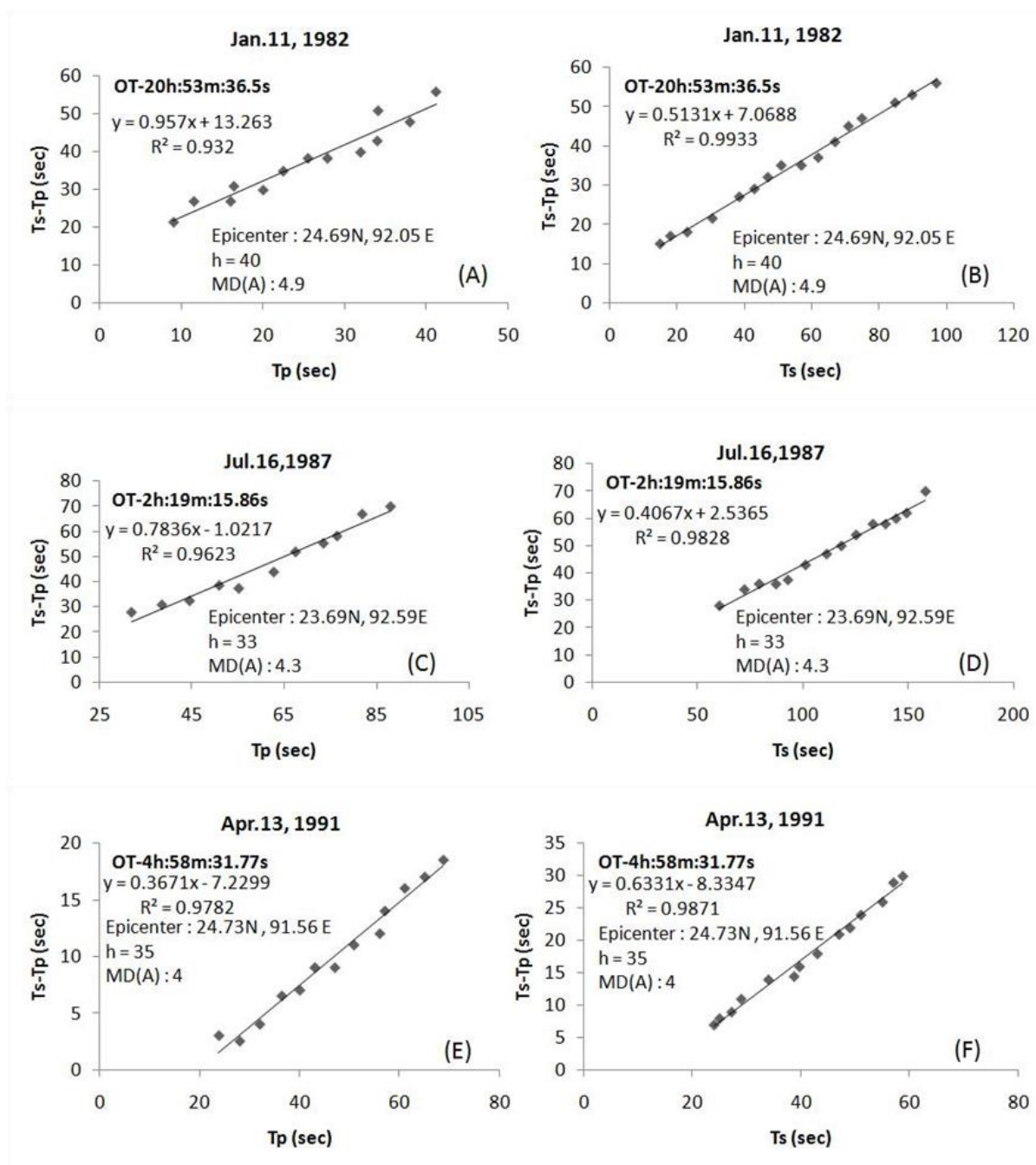


Figure 4. Wadati diagrams (A, B, C, D, E and F) for the earthquakes associated with events in the eastern part of Surma valley at depths (h) ranging between 21-40 km. Ts-Tp versus Tp and Ts-Tp versus Ts denote interval between the arrival time of P- and S-waves and arrival time of P- and S-waves at a seismic station respectively. Linear relations for the determination of P and S wave at a specific depth, involving Ts-Tp/Tp, Ts-Tp/Ts and origin time (O.T) are also shown.

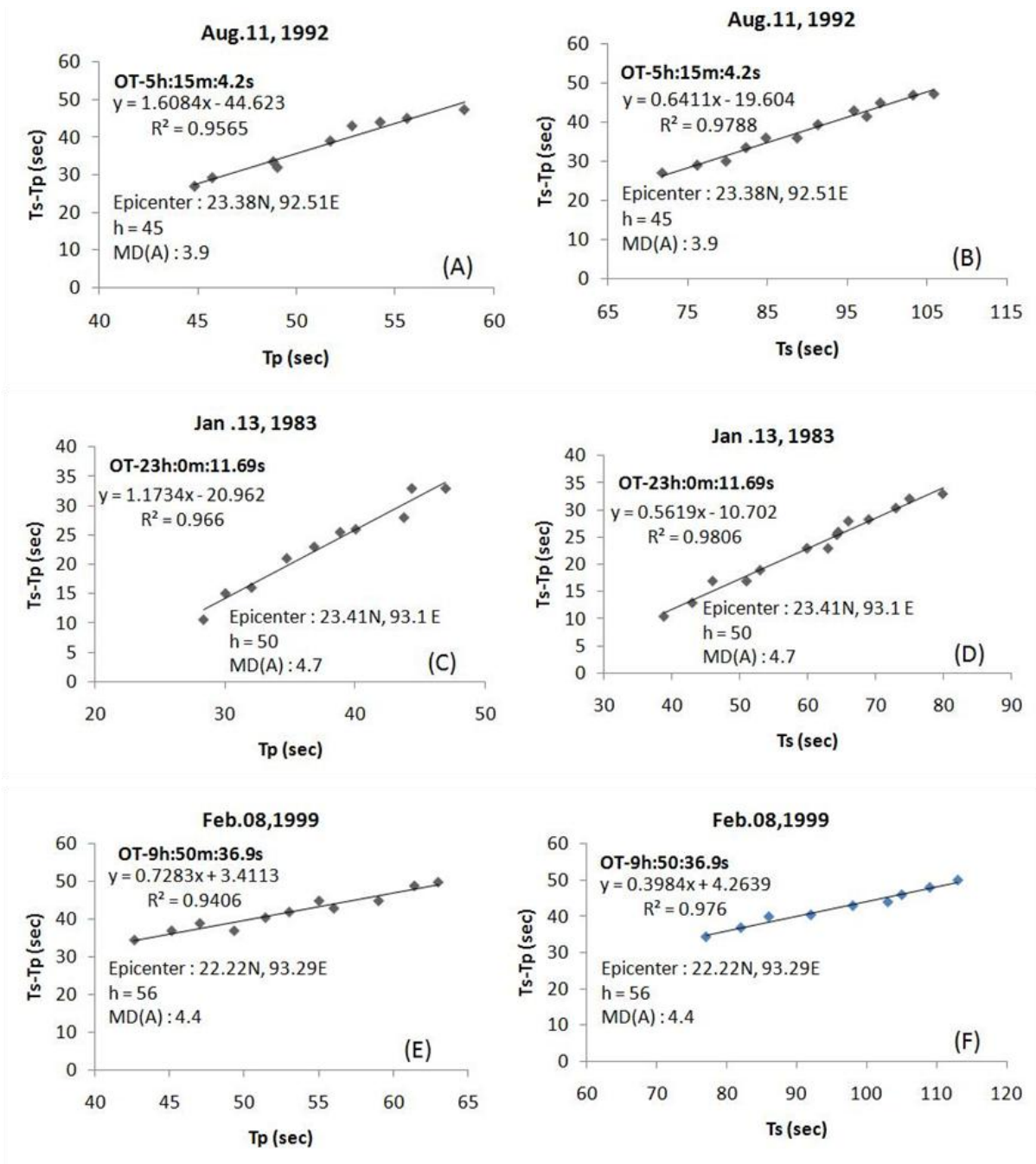


Figure 5. Wadati diagrams (A, B, C, D, E and F) for the earthquakes associated with the events in the eastern part of Surma valley at depths (h) between ranging between 41-60 km. Ts-Tp versus Tp and Ts-Tp versus Ts denote interval times of P- and S-waves and arrival time of P- and S-waves at a seismic station respectively. Linear relations for the determination of P- and S-wave at a specific depth, involving Ts-Tp/Tp, Ts-Tp/Ts and origin time (O.T) are also shown.



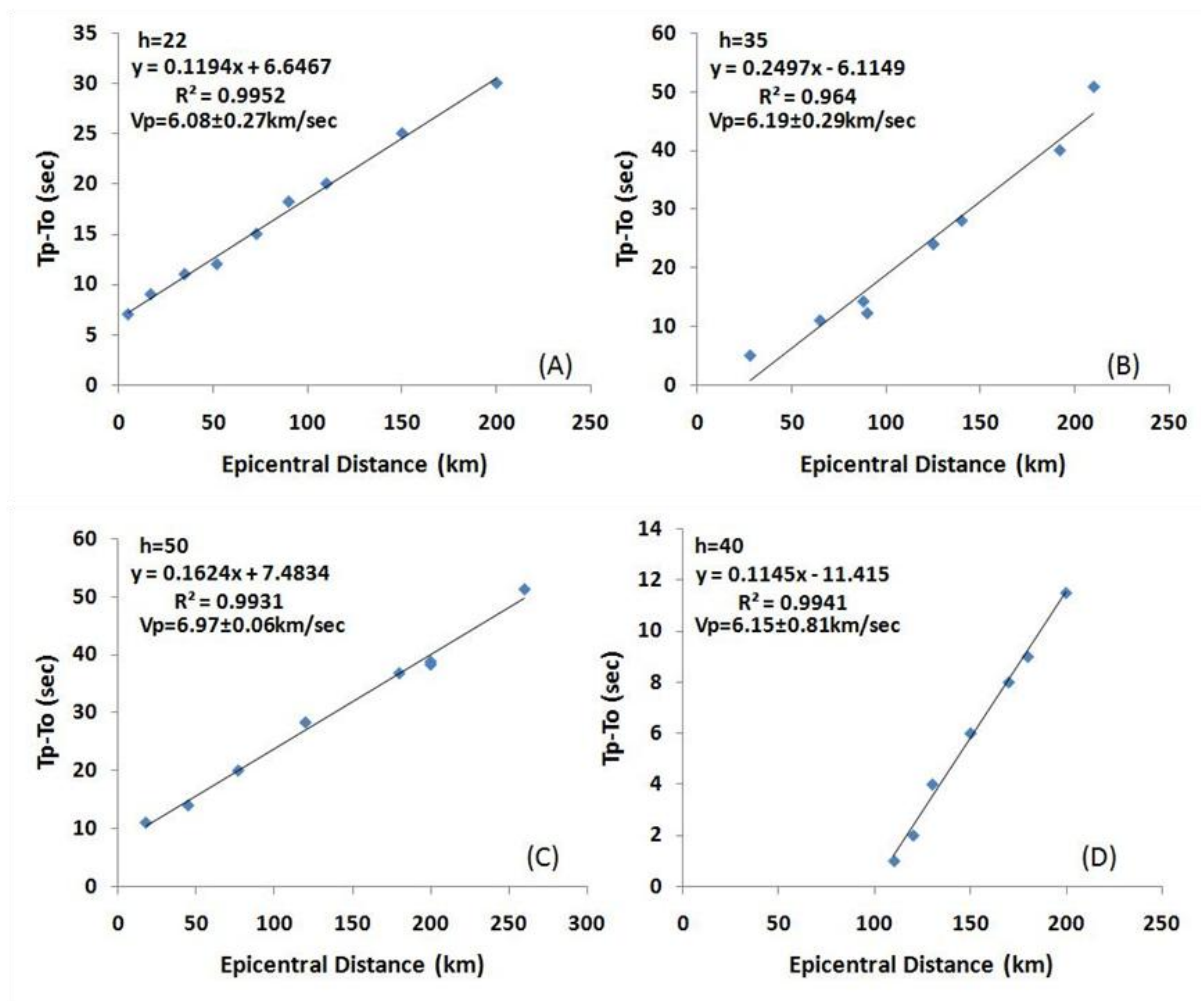


Figure 6. Ryznichenko diagrams (A, B, C and D) of earthquakes associated with events in the eastern part of Surma valley as recorded in different selected seismic stations in the northeast. Linear relation between  $T_p - T_o$  and epicentral distance (+) are also shown for the events at different depth ranges.

values remains within 25-35 sec interval exclusively for two numbers of events (A B and CD) with less deviation from the linearity while  $T_s - T_p$  values lie within 10-40sec interval for the same two numbers of events (E and F) with higher deviation from the linearity. Less variation is observed when compared with the travel time of P-wave while higher variation of  $T_s - T_p$  is reflected when plotted with respect to travel time of S i.e.  $T_s$ . In this case, the Wadati plots have been carried out up to the depth range 7 to

20 km. Magnitudes for all these events are above 4.5.

Similarly, same trend is observed in case of the Wadati plot for eastern part of Surma valley and its vicinity as illustrated in the Figure 4 and 5, where a different depth range up to 40 km and 56km is considered respectively.

Simultaneously, the Ryznichenko diagrams of earthquakes associated with events in the eastern part of Surma valley (Figure 6) are plotted against various depth intervals. All the plots

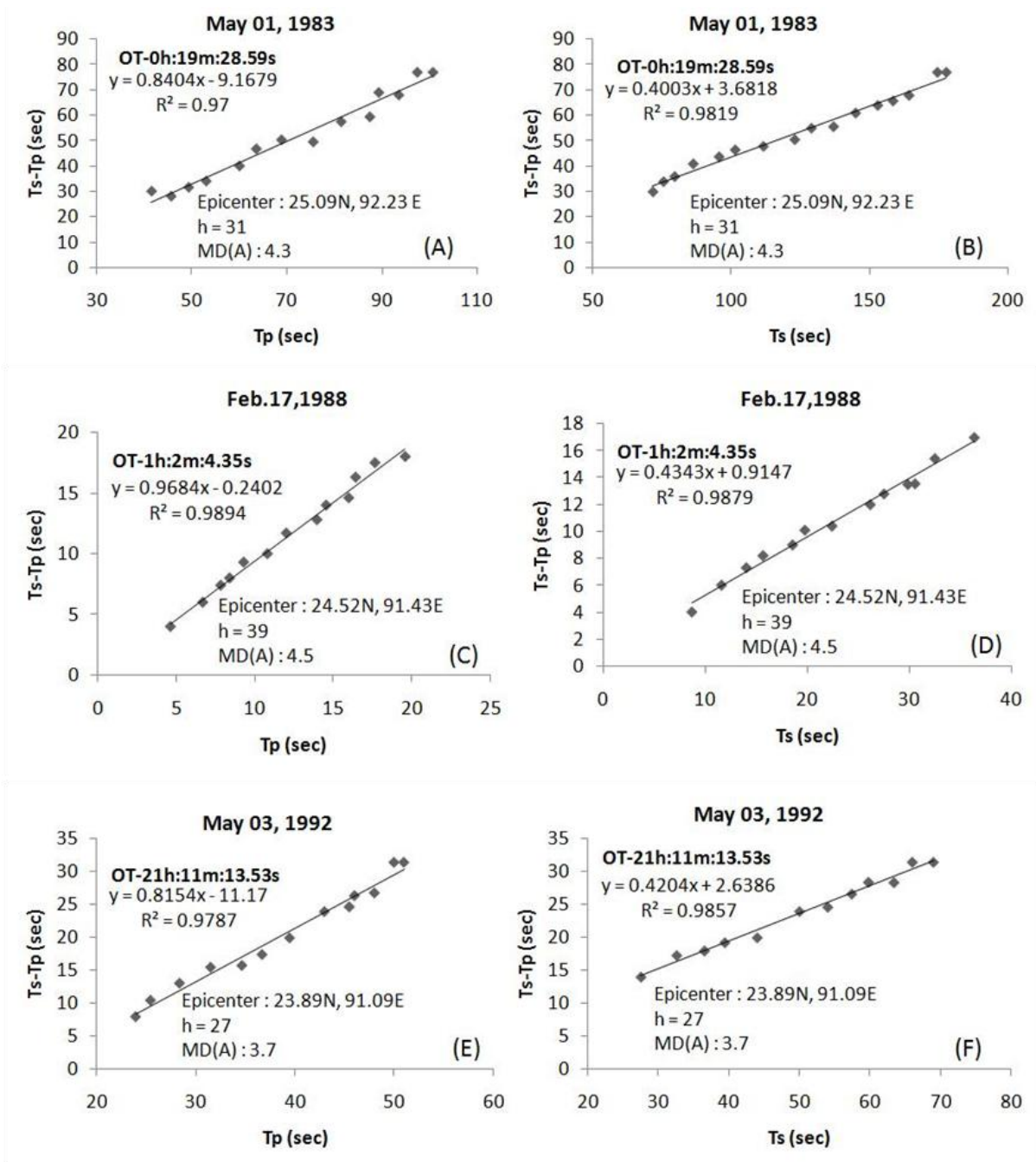


Figure 7. Wadati diagrams (A, B, C, D, E and F) for the earthquakes associated with events in the northern part of Surma valley at depths (h) ranging between 21-40 km. Ts-Tp versus Tp and Ts-Tp versus Ts denote interval between the arrival time of P- and S-waves and arrival time of P- and S-waves at a seismic station respectively. Linear relations for the determination of P- and S-wave at a specific depth, involving Ts-Tp/Tp, Ts-Tp/Ts and origin time (O.T) are also shown.

Estimation of travel time of P- and S-waves in and around Sylhet and Mat faults in Surma Basin

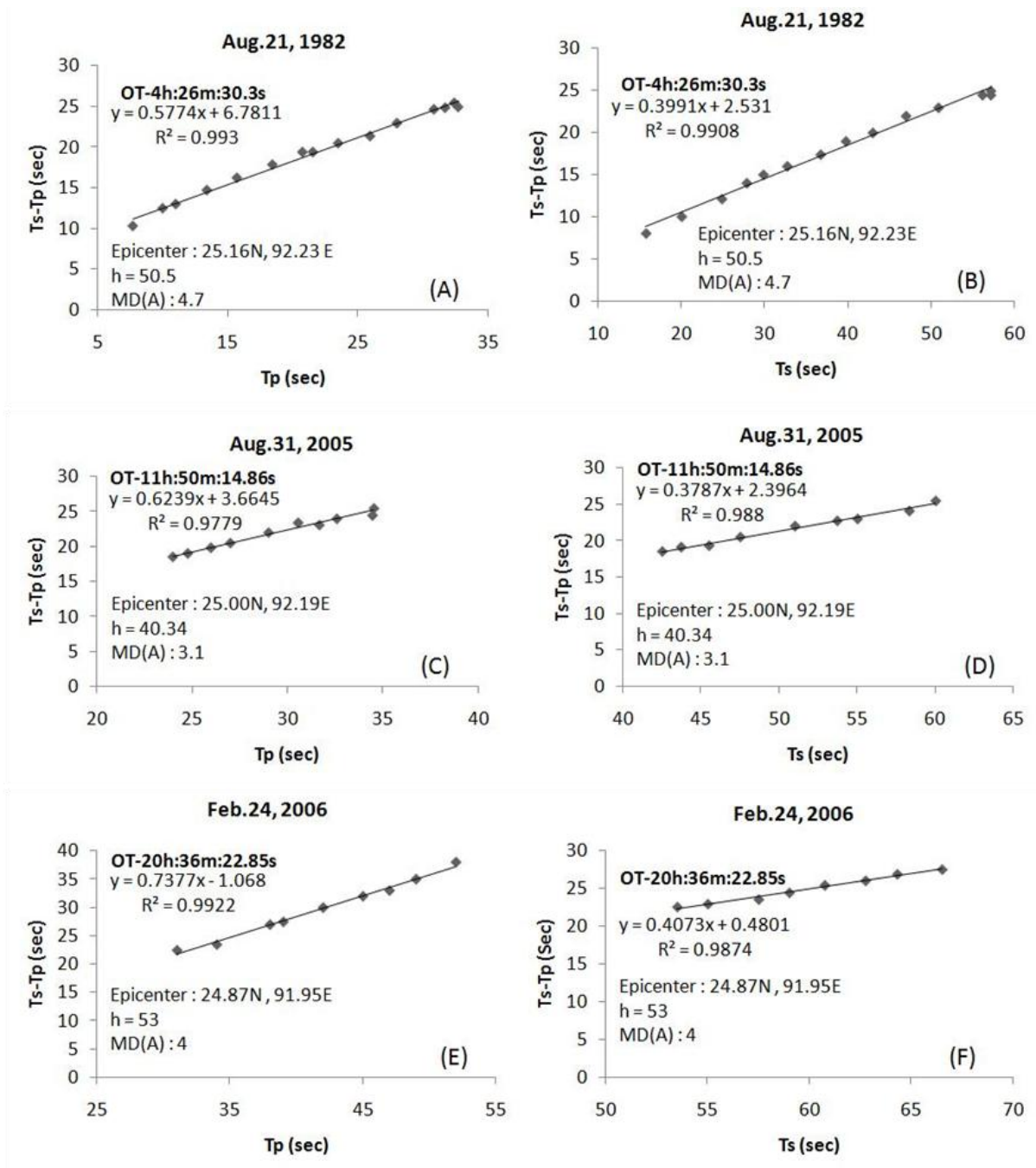


Figure 8. Wadati diagrams (A, B, C, D, E and F) for the earthquakes associated with events in the northern part of Surma valley at depths (h) ranging between 41-60 km. Ts-Tp versus Tp and Ts-Tp versus Ts denote interval between the arrival time of P- and S-waves and arrival time of P- and S-waves at a seismic station respectively. Linear relations for the determination of P- and S-wave at a specific depth, involving Ts-Tp/Tp, Ts-Tp/Ts and origin time (O.T) are also shown.

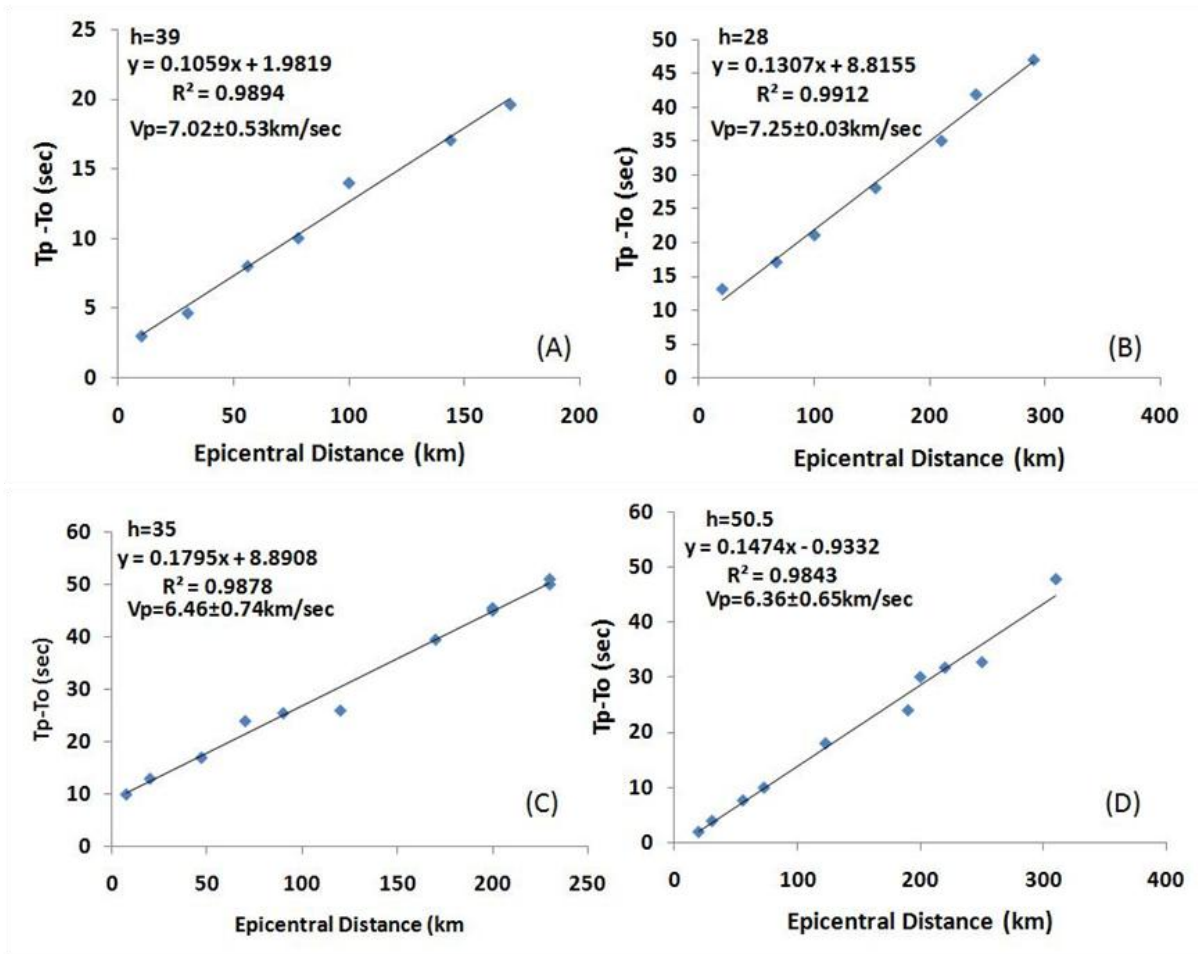


Figure 9. Riznichenko diagrams (A, B, C and D) of earthquakes associated with events in the northern part of Surma valley as recorded in different selected seismic stations in the northeast. Linear relation between  $T_p - T_o$  and epicentral distance (+) are also shown for the events at different depth ranges.

indicate clear dependence of S-P travel time ( $T_s - T_p$ ) with respect to epicentral distance (D). Interestingly, the S-P travel time does not vary much up to the depth range of 20 km with the increase in epicentral distances. However S-P travel time ( $T_s - T_p$ ) is found to be larger with the increase of epicentral distance (D) exclusively for the depth range interval of 21-40 km.

For northern part of Surma valley, similar Wadati and Riznichenko diagrams are plotted in order to ascertain the travel times used to learn about the velocity of P-wave and S-wave of the structure within the source and the re-

ceiver. Since Wadati diagram depends only on the observed arrival times of P- and S-waves, Figure 7 allows to observe the dependence of arrival time on the epicentral distances. The plots indicate no other dependence on any other parameters out of hypocentral parameters. No significant change in dependence of depth is observed except some more linearity dependence in the depth range of 41-60 km. The station wise plots however indicate the dependency of site characteristics of the particular station which is well reflected in the plots. There are some inconsistencies in the plots which might be

due to the heterogeneous site pertaining to each station. Otherwise the trend, as observed and explained in Figure 6, remains the same.

The internal consistency of the data suggests that these values are useful as estimates of the first order variation in velocity structure and can be used to improve the velocity model used for location. For focal depths range from 7 to 40 km, the Ryznichenko diagrams clearly show the change in shape of the travel time versus distance plot with increasing focal depth, indicative of both a geometrical effect and an increasing P-wave velocity. The Wadati diagrams show a systematic decrease in  $t_s/t_p$ , suggesting that the velocity for shear waves increases faster than that for the compressional waves in the upper part of the crust. Simultaneously, the nonlinearity of the Wadati diagram indicate that  $t_s/t_p$  indeed changes with depth and it could be established that the diagram more or less resolve the plot.

## CONCLUSIONS

The study deals with the estimation of travel times of P- and S-waves in Surma Basin. It is to be noted that lower crustal activity was very less in the study region prompting relocation of earthquake events. The relocation of events has considerably lowered the error pertaining to latitude, longitude and depth. The relocated events become an input to the study (Fig. 1). In this study, it is observed that  $T_s$ - $T_p$  is varying with depth and considerably possesses some dependence of  $T_p$  and  $T_s$  on depth. Additionally, it is observed that  $t_s/t_p$  also decreases with depth, this implies that similar variation in velocity of P, velocity of S requires separate velocity structure for P and S if really accurate hypocentral parameters are required to be worked out. Several other studies<sup>19</sup> also find similar results. With the advent of digital data and the increasing use of three component stations, large number of good quality S-waves arrival are being recorded by micro earthquake networks. These S-wave arrivals require proper modeling if full advantage is to be taken of the increase resolution such

as secondary arrivals can provide. In this study, accurate phase picking on P- and S-wave arrivals and subsequent locations no doubt contributed in a large way towards the travel time estimations. The simple geometries involved in the Ryznichenko diagram were first discussed by Green<sup>20</sup> although the semi-log form of presentation for using velocities determinations in earthquake focal depth was developed by Ryznichenko. The study, first of its kind in this basin, may be further improved with the establishment of a new seismological network, having the azimuthally coverage of both the faults which is the scope of further study.

## ACKNOWLEDGEMENTS

Finance assistance received from Department of Science & Technology, vide grant no. DST/23(194)/ESS/99 to RPT is thankfully acknowledged. The authors acknowledge the organizations namely, CSIR-NEIST Jorhat, CSIR-NGRI Hyderabad, Manipur University, IMD New Delhi and Gauhati University for its contribution in terms of earthquake data which has paved the way for this study. The first author takes the opportunity to thank Director, CSIR-NEIST, Jorhat, for the help rendered to carry forward the work.

## REFERENCES

1. Stein S & Wysession M (2003). *An Introduction to Seismology, Earthquakes, and Earth Structure*. Blackwell Publishing, Ltd., Massachusetts, USA, pp. 199–161.
2. Tandon AN (1954). A study of Assam earthquake of August 1950 and its aftershocks. *Indian J Met Geophys*, **5**, 95–137.
3. Saha SN, Gaur VK, Bansal V, Wyss M & Khattri, K (1981). Microearthquakes in North East India. Symp. *Earthq. Disaster Mitigation, March 4-6, 1981, Univ. Roorkee, Roorkee (India)*, **2**, 65–76.
4. Gupta HK, Singh SC, Dutta TK & Saikia MM (1982). Seismicity studies in Northeast India. *Proc. Symp. Seismicity and Microzonation, Seattle, Washington*.
5. Joyner WB & Boore DM (1981). Peak horizontal acceleration and velocity from strong-motion records including records from the 1979 Imperial Valley, California,

- earthquake. *Bull Seism Soc Am*, **71**, 2011–2038.
6. Bullen KE (1947). *An Introduction to the Theory of Seismology*. Cambridge University Press, New York, USA, pp. 249–253.
  7. Jeffreys H & Bullen KE (1940). *Seismological Tables*. British Association for the Advancement of Science, Gray Milne Trust, London, UK, pp. 1–48.
  8. Tiwari RP (2002). Status of seismicity in the Northeast India and earthquake disaster mitigation. *Envis Bulletin Him Eco Dev*, **10**, 10–21.
  9. Sailo S, Tiwari RP & Baruah S (2011). Seismotectonics of Surma basin with special reference to Sylhet and Mat faults. *Mem Geol Soc India*, **77**, 185–193.
  10. Nandy DR (2001). *Geodynamics of Northeastern India and the adjoining region*. ACB publications, Kolkata, India, pp. 96–106.
  11. Lienert BR, Berg E & Frazer LM (1986). HYPOCENTER: An earthquake location method using centered, scaled and adaptively damped least squares. *Bull Seism Soc Am*, **76**, 771–783.
  12. Bhattacharya PM, Pujol J, Majumdar RK & Kayal JR (2005). Relocation of earthquakes in the northern region using joint hypocentre determination method. *Curr Sci*, **89**, 1404–1413.
  13. Wadati K (1933). On the travel time of earthquake waves. *Geophys Mag*, **2**, 101–111.
  14. Riznichenko YV (1958). Methods for large-scale determination of focus coordinates of nearby earthquakes and velocities of seismic waves in the focal region. *Tr Inst Fiz Zemli Akad Nauk SSR*, **4**.
  15. Bune VI, Gzovskiy MV, et al. (1960). Methods for a detailed study of seismicity. *Izv Acad Sci USSR, Trudy*, **9**, no. 176, 327 (in Russian).
  16. Khattri KN, Wyss M, Gaur VK, Saha SN & Bansal V (1983). Local seismic activity in the region of Assam gap, NE India. *Bull Seism Soc Am*, **73**, 459–469.
  17. Nicholson C & David WS (1985). *Bull Seism Soc Am*, **75**, 1105–1123.
  18. Kisslinger C & Engdahl ER (1973). The interpretation of the Wadati diagram with relaxed assumptions. *Bull Seism Soc Am*, **63**, 2176–2176.
  19. Archuleta RJ (1982). Analysis of near source static and dynamic measurements from the 1979 Imperial Valley earthquake. *Bull Seism Soc Am*, **72**, 1927–1956.
  20. Green CH (1938). Velocity determinations by means of reflection profiles. *Geophysics*, **3**, 295–305.